Monthly Notices
of the
ROYAL ASTRONOMICAL SOCIETY

MNRAS **448,** 1199–1205 (2015) doi:10.1093/mnras/stv003

On-sky tests of the CuReD and HWR fast wavefront reconstruction algorithms with CANARY

Urban Bitenc,[1]⋆ Alastair Basden,[1] Nazim Ali Bharmal,[1] Tim Morris,[1] Nigel Dipper,[1] Eric Gendron,[2] Fabrice Vidal,[2] Damien Gratadour,[2] Gérard Rousset[2] and Richard Myers[1]

[1] *CfAI, Department of Physics, Durham University, South Road, Durham DH1 3LE, UK*
[2] *LESIA, Observatoire de Paris, 5 Place Jules Janssen, F-92190 Meudon, France*

Accepted 2014 December 25. Received 2014 December 23; in original form 2014 December 10

ABSTRACT

CuReD (Cumulative Reconstructor with domain Decomposition) and HWR (Hierarchical Wavefront Reconstructor) are novel wavefront reconstruction algorithms for the Shack–Hartmann wavefront sensor, used in the single-conjugate adaptive optics. For a high-order system they are much faster than the traditional matrix–vector-multiplication method. We have developed three methods for mapping the reconstructed phase into the deformable mirror actuator commands and have tested both reconstructors with the CANARY instrument. We find out that the CuReD reconstructor runs stably only if the feedback loop is operated as a leaky integrator, whereas HWR runs stably with the conventional integrator control. Using the CANARY telescope simulator we find that the Strehl ratio (SR) obtained with CuReD is slightly higher than that of the traditional least-squares estimator (LSE). We demonstrate that this is because the CuReD algorithm has a smoothing effect on the output wavefront. The SR of HWR is slightly lower than that of LSE. We have tested both reconstructors extensively on-sky. They perform well and CuReD achieves a similar SR as LSE. We compare the CANARY results with those from a computer simulation and find good agreement between the two.

Key words: instrumentation: adaptive optics – methods: numerical – methods: observational – techniques: high angular resolution.

1 INTRODUCTION

Image quality in ground-based astronomy is strongly affected by the wavefront distortions introduced by atmospheric turbulence. Adaptive optics (AO; first proposed by Babcock 1953, for an overview see Davies & Kasper 2012) can restore diffraction limited images by sensing the distortions and correcting them with a deformable mirror (DM) in real time. A Shack–Hartmann (SH) wavefront sensor (WFS) measures wavefront gradients averaged over small sections of the pupil, called subapertures. Traditionally, the DM commands are calculated by multiplying a vector of gradients with a control matrix (matrix–vector multiplication, MVM).

The proposed extremely large telescopes (ELTs) will have mirror diameters up to 39 m (de Zeeuw, Tamai & Liske 2014). Recently, Basden & Myers (2012) have shown that with sufficient computing power it is possible to use MVM with almost all AO systems on the European ELT (Spyromilio et al. 2008). However, for the proposed instrument EPICS (Kasper et al. 2010) this will most likely not be possible (control matrix size 60 000 × 30 000, update rate of a few kHz). The required matrix inversion could also be challenging. This led to a development of a number of faster methods for wavefront reconstruction as summarized by Zhariy et al. (2011). A more efficient method might be preferable even for AO systems that can be controlled by MVM, since that would cut costs on hardware, power and cooling. Furthermore, a high-order laboratory AO system or a computer simulation would benefit significantly from a fast reconstructor that achieves a high-speed correction without an expensive computer cluster.

CuReD (Cumulative Reconstructor with Domain decomposition, see Zhariy et al. 2011; Rosensteiner 2012) and HWR (Hierarchical Wavefront Reconstructor, Bharmal et al. 2013) are two examples of such fast algorithms. They are used in close-loop for the single-conjugate AO with the Fried geometry, where the DM actuators coincide with the subaperture corners of the WFS. They reconstruct the wavefront from the slope measurements, but do not provide the DM commands. In this work, we develop three methods for mapping the CuReD or HWR output into DM commands. This needed to be done so the algorithms could be used on a real AO system. We tested both algorithms thoroughly with the CANARY instrument (Myers et al. 2008), using its Telescope Simulator (TelSim). The main purpose of this work is to report the successful on-sky

⋆ E-mail: urban.bitenc@durham.ac.uk

tests of CuReD and HWR with CANARY. It is crucial to test new algorithms on-sky to expose them to the variability of the atmosphere and to other effects that are not accounted for in simulations, and recently also other algorithms have been tested on-sky using CANARY (Gendron et al. 2011; Osborn et al. 2014; Sivo et al. 2014). For comparison and further investigation we also studied CuReD and HWR using a computer simulation.

Since 2013 another fast wavefront reconstructor has been successfully used on-sky (Poyneer et al. 2014): the Fourier Transform Reconstructor (FTR, see Poyneer, Gavel & Brase 2002) is used in the Gemini Planet Imager (Macintosh et al. 2014). Compared to FTR, CuReD may computationally be even faster and perhaps less sensitive to misalignment.

We presented our initial measurements at the AO4ELT3 conference (Bitenc et al. 2013), hinting that in some cases CuReD provides a higher SR than the least-squares estimator (LSE). After a thorough investigation we here provide an explanation for this unexpected result.

Since CANARY is a low-order system, we cannot fully study the main concern with CuReD and HWR: the noise propagation. Noise and the speed-up of the algorithms remain to be investigated in the future on higher-order systems.

2 CONTROL METHODS

In this section, we describe the methods used to calculate the DM commands from the measured wavefront gradients, i.e. to control the DM based on the input from the WFS. The wavefront correction was carried out in closed-loop, with the WFS observing only the residual wavefront aberration after the correction.

2.1 Least-squares estimator

The established method of controlling the DM is via an MVM, see e.g. Boyer, Michau & Rousset (1990). We obtained the control matrix as a pseudo-inverse of the system's interaction matrix (WFS response to DM commands), using singular value decomposition (SVD). This control method is referred to as an LSE. We optimized the number of modes in the matrix inversion: for the real CANARY system we rejected 6 modes (out of 54) with the smallest singular values, whereas in the simulation it was optimal to reject 2 modes (out of 52, as our simulation has no tip–tilt mirror). Alternative methods can be used to obtain the control matrix for MVM, as we note in Section 5.

LSE was used as the figure of merit for CuReD and HWR performance.

2.2 CuReD and HWR algorithms

When using CuReD or HWR, the calculation of the actuator commands is performed in two independent steps: wavefront reconstruction and wavefront-to-actuator mapping.

2.2.1 Wavefront reconstruction

CuReD and HWR are used with the SH WFS. With an additional pre-processing step they can also be used with the pyramid WFS (Shatokhina et al. 2013). Their basic principle is to reconstruct the wavefront by 'integrating' (i.e. summing up) the wavefront gradients. CuReD sums up gradients along horizontal and vertical lines (left plot of Fig. 1), whereas HWR sums them up along diagonal

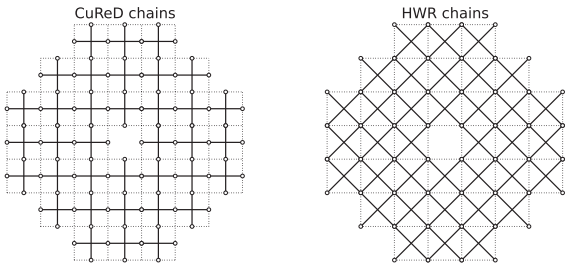

Figure 1. CANARY subapertures (dotted lines) with the lines along which CuReD (left) and HWR (right) sum up gradients. Empty circles are the points at which the wavefront values are calculated by summing up gradients. For HWR these points coincide with the actuator positions, whereas CuReD needs an additional step to calculate the output values according to the Fried geometry.

lines (right plot of Fig. 1); for more details see Rosensteiner (2012) and Bharmal et al. (2013). The number of floating point operations for CuReD is $20n$ and for HWR it is $O(n^{3/2})$, where n is the number of subapertures.

Summing up of gradients results in bad noise propagation properties, particularly for large AO systems where the gradient chains would be very long. The algorithms address this issue by splitting the pupil into smaller *domains* where the wavefront reconstruction is applied and afterwards the partial wavefronts are recombined into the global wavefront. However, using a computer simulation we confirmed that on a system with 7×7 subapertures CuReD and HWR are affected by noise only slightly more than the MVM, hence the efficiency of this approach could not be studied.

Using the domains it is also straightforward to account for the central obscuration or any other excluded subapertures, as long as the used subapertures are all connected. In our tests the CuReD wavefront was composed of four domains to account for the central obscuration. For HWR we set the weight mentioned in section 3.3 of Bharmal et al. (2013) to 2.0; the simulation described in Section 3.1 confirmed that this is the optimal value.

Using CuReD we found out that its reconstructed wavefront is slightly smoothened and the high spatial frequencies are attenuated. This is demonstrated in Fig. 2 which shows the CuReD response to a poked actuator. An exact algorithm reconstructs the input actuator commands perfectly, whereas CuReD broadens the peak. The source of this broadening could be the averaging performed in the last step of CuReD (Rosensteiner 2011, section 3, equation 16– 20). It seems that this property crucially impacts the CuReD

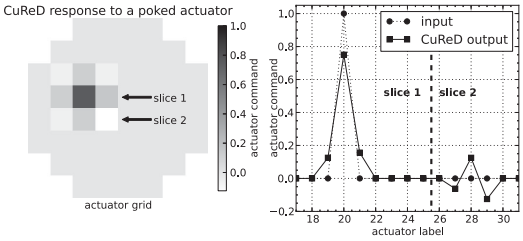

Figure 2. CuReD response to slopes resulting from a poked actuator in simulation using the bilinear DM interpolation. The left plot shows the CuReD output on a two-dimensional actuator grid. The squares in the right plot show the same data plotted in one dimension for the selected two rows of actuators (slice 1 and 2). An ideal reconstructor would exactly reproduce the input actuator commands represented by the circles on the right plot. In contrast to that, CuReD output exhibits a significant widening of the input peak.

performance and stability. HWR does not exhibit this effect; it can even be configured in such a way that in simulation a poked actuator is reproduced *exactly*.

The output of this step are the wavefront values at subaperture corners in arbitrary units.

2.2.2 *Wavefront-to-actuator mapping*

In the second step, these wavefront values are used to calculate the actuator commands. We developed and investigated three ways of doing this: we call them *identity mapping*, *interpolation mapping* and *full mapping*.

Identity mapping maps the wavefront values directly to the corresponding actuators and accounts only for the phase-to-voltage scaling for each actuator. To obtain the scaling, the slopes obtained by poking an actuator are fed into CuReD or HWR and the peak value of the reconstructed wavefront is inverted. This is the simplest and fastest mapping, the number of computing operations being N (number of actuators).

Interpolation mapping additionally accounts for potential misalignment between the DM and the SH lenslet array. For this method, the actuator positions w.r.t. subaperture corners are determined in advance by the method described in the appendix. The wavefront values at the actuator positions are obtained from the CuReD or HWR output by bilinear interpolation (extrapolation if outside the grid). These interpolated values are then scaled to obtain actuator voltages in the same way as for the identity mapping. The number of operations is $7N$.

Full mapping additionally accounts for any other experimental effects like interactuator coupling, reconstructor's response function, partial illumination of subapertures, etc. It is performed by multiplying the CuReD or HWR output with the so-called *mapping matrix*, which is obtained in the following way. Each column of the interaction matrix (i.e. the measured gradients for each poked actuator) is processed by CuReD or HWR and the output is stored in the corresponding column of another matrix. This matrix is then inverted using SVD to obtain the mapping matrix; for the real CANARY system we typically rejected four modes for CuReD and one mode for HWR. The number of computing operations for this method is $N(2N - 1)$, so it is as slow as MVM and cannot be used on high-order systems such as ELTs. We only deployed it for its simplicity and as the figure-of-merit for the other two methods.

Apart from the DM, CANARY also has a tip–tilt mirror. Offloading tip–tilt happens automatically in the case of full mapping. For identity and interpolation mapping we subtract a fitted plane from the CuReD or HWR output; from the slope of the plane we calculate the commands for the tip–tilt mirror. This can be done in $8N + 2$ operations. Alternatively, one could subtract the average slopes from the CuReD or HWR input.

Importantly, the total number of operations for the identity and interpolation mapping is a linear function of N.

3 EXPERIMENTAL SETUP

CANARY is an instrument that was developed to provide the first on-sky demonstration of the technique of Multi-Object AO. For the tests presented in this paper it was operated in its basic closed-loop Single-Conjugate AO mode. In this mode, it uses a single on-axis closed-loop WFS with 7×7 subapertures of which 36 are illuminated and used to measure wavefront gradients. The DM has 52 controlled actuators in an 8×8 array, and the tip–tilt mirror has two actuators. The actuator voltages were updated with a frequency of 150 Hz. The lenslet array and the DM are aligned in the Fried geometry.

CANARY comprises a TelSim which uses rotating phase-screens to simulate the effects of the atmosphere and creates the turbulence-distorted point-spread-function in the focal plane of the telescope. The NGS light source was set to a high level (1500 photons per WFS pixel) so we could study the algorithms in the low-noise regime.

The use of the TelSim was essential because, unlike with the real atmosphere, its Fried parameter r_0 stays constant in time. This enabled us to optimize the settings (loop gain and conditioning factors in matrix inversion), study the mapping methods and compare the Strehl ratios for different control algorithms. However, a repeatability test showed that even when using TelSim the SR can change by several per cent over a range of 10 min. Therefore, we performed all comparisons by repeating the measurements several times in an interleaved manner ('ababab' rather than 'aaabbb').

For the real-time control (RTC) CANARY uses the Durham AO Real-time Controller, DARC (Basden & Myers 2012). Due to its dynamic loading of libraries it was possible to switch between different control algorithms within fractions of a second.

The on-sky measurements presented in this paper were taken with CANARY on the William Herschel Telescope at Observatorio del Roque de los Muchachos, La Palma, Canary Islands. The diameter of the telescope's primary mirror is 4.2 m.

3.1 Computer simulation

We simulated CANARY with the Durham AO simulation platform (DASP, Basden et al. 2007). We used DASP to simulate the atmosphere, the telescope, the WFS and the DM, but for the RTC DASP was linked with DARC in a manner described by Basden (2014). In this way it was possible to use the same RTC code in the simulation and with the real CANARY system which was extremely helpful when investigating unexpected behaviour we sometimes observed.

Simulation settings: update frequency is 250 Hz, the aperture mask for the WFS is similar as in CANARY, $r_0 = 20$ cm, outer scale is 30 m, loop gain is set to 0.5. Strehl ratios are given for wavelength of 1650 nm and are averaged over 38 s. The random seed for the generation of atmospheric disturbances was fixed so that for all the results presented the disturbances were exactly the same. The simulation does not include the tip–tilt mirror; the DM corrects also tip and tilt. The DM and the SH lenslet array are perfectly aligned. Hence, for CuReD and HWR in simulation we did not perform tests with interpolation mapping, as they would yield the same results as tests with identity mapping. The goal of these tests was to study the algorithms in the low-noise regime; therefore, we set the photon flux to a very high value. We used bicubic DM interpolation for all the results shown in this paper. We cross-checked all results with a bilinear and Gaussian DM interpolation; while the SR values depend on the DM interpolation used, all three methods reveal the same trends and lead to the same conclusions.

4 RESULTS

4.1 Loop stability

With the full mapping, both CuReD and HWR ran stably in closed loop both in the computer simulation and on CANARY. However, with the identity or interpolation mapping, we found out that CuReD runs stably for about 10–100 s after closing the loop, but afterwards the 'waffle mode' gradually spreads over the DM and some actuator

commands may reach the maximum or minimum allowed values. The AO correction deteriorates and the loop eventually becomes unstable. We observed this effect in the simulation and with CANARY, both using the TelSim and on-sky.

In the simulation, we found out that this instability has two causes: partial illumination of subapertures and interactuator coupling (i.e. non-zero slopes in subapertures other than the four subapertures around the poked actuator). If in simulation all subapertures are fully illuminated and the bilinear interpolation is used for the DM (no interactuator coupling), the loop remains stable. How quickly the loop becomes unstable depends on the loop gain, but also for low gain (e.g. 0.1) it eventually becomes unstable.

The solution to this problem is to introduce a parameter α to the control loop:

$$v(t + \Delta t) = \alpha \cdot v(t) + g \cdot \Delta v(t), \quad (1)$$

where $v(t)$ are the actuator commands, $\Delta v(t)$ is the CuReD output, g is the loop gain and α is the *decay factor*. This type of control loop is called 'leaky integrator'. We found out that lowering α from the default value of 1.0 to a value of 0.99 stabilizes the loop: it ran stably for over an hour in simulation with $g = 0.9$, and for over half an hour with the CANARY TelSim with $g = 0.5$. For all results in this paper a value of $\alpha = 0.99$ was used for the CuReD reconstructor when used with the identity or interpolation mapping; in all other cases a value $\alpha = 1.0$ was used.

In simulation, we found that for any reconstructor the SR is slightly dependent on α. The behaviour depends on the DM interpolation method used, as shown in Fig. 5.

Unlike CuReD, HWR runs stably using identity mapping or interpolation mapping also with $\alpha = 1.0$.

4.2 CuReD and HWR performance dependence on the mapping method used

We used CANARY TelSim to investigate how the SR achieved with CuReD and HWR depends on the mapping method used.

Between the HWR and CuReD tests CANARY was realigned. On average the fitted actuator positions were $0.09a$ away from the subaperture corners for the tests of HWR and $0.15a$ for CuReD; the furthest one was $0.22a$ away for HWR and $0.28a$ for CuReD, where a is the length of the subaperture side. We optimized the gain and the number of modes rejected in the matrix inversion for the full mapping. The obtained Strehl ratios are presented in Table 1, together with the results of the computer simulation.

The key result is that both CuReD (with $\alpha = 0.99$) and HWR run stably with the identity and interpolation mapping, and with little loss in performance; for CuReD the SR is even higher than with the full mapping. This is essential for the use of these algorithms on an ELT or other high-order systems because it guarantees that the mapping of the CuReD or HWR output to the DM commands can be done fast enough.

The fact that the performance is good with both identity and interpolation mapping shows that the mapping is robust, since the assumed actuator positions are up to $0.28a$ apart for the two (see Fig. A1). For CuReD one can see an improvement of the interpolation mapping over the identity mapping, presumably because the wavefront values are calculated at the more accurate actuator positions. For HWR one cannot see this effect.

Computer simulation agrees well with the results from CANARY TelSim.

4.3 Performance comparison: CuReD and HWR versus LSE

In the computer simulation the Strehl obtained by CuReD is higher than that of LSE, and the Strehl of HWR is lower (Tables 1 and 2; see also Fig. 5). We have investigated the validity of this result and we find that it is independent of:

(i) the mapping method used for CuReD and HWR (identity mapping, full mapping),
(ii) interpolation method used for the DM (bilinear, Gaussian, bicubic),
(iii) loop gain,
(iv) factor α,
(v) illumination of subapertures (fully illuminated or with a realistic CANARY-like illumination),
(vi) r_0 (20 cm, 60 cm),
(vii) the use of a spatial filter (used or not used).

We used CANARY TelSim (with optimized gains and the conditioning parameters in matrix inversions) to compare the performances of LSE, CuReD and HWR, the latter two using the full mapping. The results are summarized in Table 2: unlike in the simulation, LSE achieves the highest SR, followed by CuReD and HWR.

Next, we lowered the intensity of the TelSim light source to increase noise; the brightest pixel in the WFS got about 30 photons. As shown in the third line of Table 2, CuReD and HWR worked well also with the lower light level.

Finally, we compared LSE with CuReD, the latter using interpolation mapping, for a number of settings (loop gain and conditioning parameter) close to the optimal ones. The results are presented in Fig. 3: in this case the Strehl ratios obtained with CuReD are at least as high as those of LSE and in several cases they are higher. This nicely agrees with the computer simulation, where CuReD achieves a higher Strehl than LSE.

Table 1. Comparison of the mapping methods in terms of the Strehl ratios they achieve. The results for CuReD and HWR obtained with the CANARY TelSim in this table are not comparable.

Strehl ratio (per cent)	'Identity'	'Interpol.'	'Full'
CuReD			
Computer simul.	31.2	–	29.8
CANARY TelSim	36.6 ± 0.3	37.3 ± 0.3	35.4 ± 0.2
HWR			
Computer simul.	27.0	–	27.0
CANARY TelSim	28.6 ± 0.2	28.7 ± 0.2	29.3 ± 0.3

Table 2. Comparison of CuReD, HWR and LSE, the latter two using full mapping. The low-noise measurement with CANARY TelSim was performed twice. With full mapping CuReD performs worse than LSE.

Strehl ratio (per cent)	LSE	CuReD 'full map.'	HWR 'full map.'
Computer simul.	29.2	29.8	27.0
CANARY TelSim			
Low noise, 1	33.5 ± 0.7	31.7 ± 0.5	29.1 ± 0.5
Low noise, 2	27.6 ± 0.4	26.7 ± 0.6	24.6 ± 0.9
Higher noise	32.3 ± 0.6	30.6 ± 0.5	27.9 ± 0.6

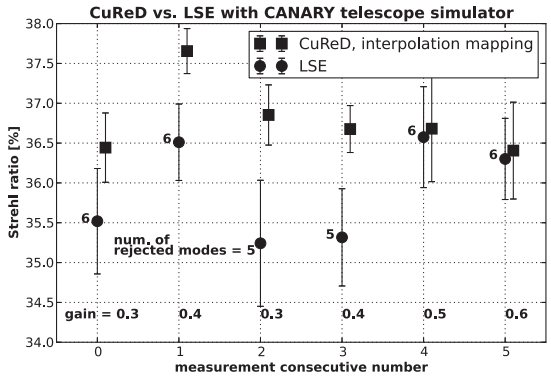

Figure 3. Comparison of CuReD with interpolation mapping and LSE, using CANARY TelSim. The values at the bottom of the plot denote the loop gain and the numbers next to the circle points denote the number of modes rejected for the LSE. With interpolation mapping CuReD performs better than LSE.

4.4 Measurements on-sky

The algorithms were tested on-sky during seven nights between 2012 October and 2014 October. We collected eight data sets using stars with magnitude around 11 and one data set with a star of magnitude about 4. The total on-sky time over all the data sets sums up to about 5 h. The individual measurements comprise between 30 and 60 s of near-infrared image data. The atmospheric conditions varied between the data sets. To be exposed to as similar atmosphere as possible, the reconstructors were tested in an interleaved manner (abcabcabc). The loop gain values were between 0.2 and 0.5.

CuReD and HWR were stable on-sky with both full and interpolation mapping. Most of the time we used the full mapping because it was the first one we implemented. We present the average Strehl ratios for each data set in Fig. 4: generally CuReD performs similarly to LSE, whereas HWR is slightly lower. The variability of the atmosphere does not make it possible to compare the Strehl ratios obtained with the two mapping methods.

The HWR results from 2012 may be affected by a mistake in off-loading tip–tilt. During the 2013 run we experimentally set a high fraction (90, 92 or 95 per cent) of the mapping matrix elements to 0; this worked well but some CuReD measurements may have been affected by the instability. However, even with these issues the reconstructors achieved good results.

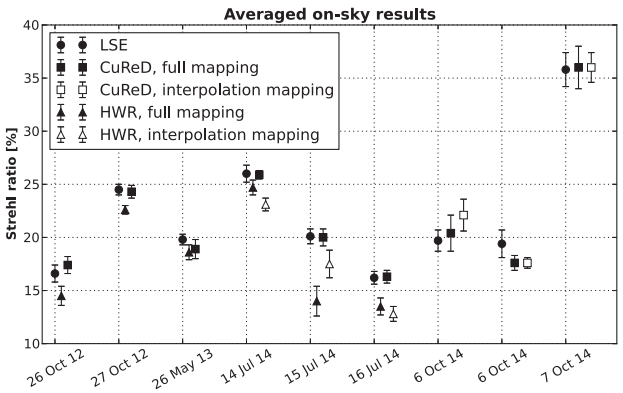

Figure 4. On-sky performance of LSE, CuReD and HWR: the average values for each of the reconstructors and for each of the nine data sets. The measurements within a data set were taken in an interleaved manner so that the reconstructors are exposed to similar atmospheric disturbances. The error bars are calculated from the standard deviations and the numbers of measurements.

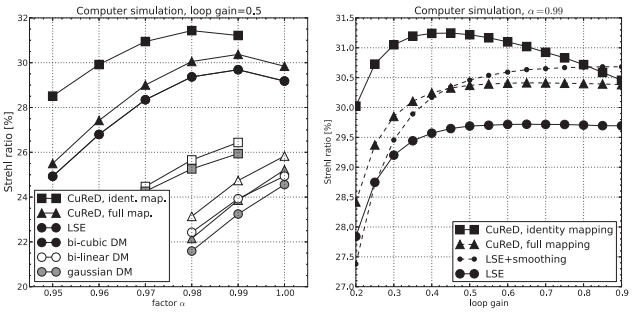

Figure 5. Strehl ratio obtained in computer simulation. Left: behaviour of the Strehl ratio with respect to the factor α depends on the DM interpolation method. As CuReD with the identity mapping is not stable for $\alpha = 1.0$, its Strehl ratio is given only for $\alpha \leq 0.99$. Right: smoothing improves the LSE Strehl (dots are higher than circles), un-smoothing lowers the CuReD Strehl (triangles are lower than squares).

5 HOW CAN CURED BE BETTER THAN LSE?

Our observations show that CuReD gives a higher SR than LSE in the low-noise regime we investigated. Rosensteiner (2012) observes the same on a simulated system with 84×84 subapertures. This is a surprising result; intuitively one expects an 'approximate' algorithm to perform worse than the 'exact' solution. How is it possible that CuReD performs better than LSE?

Two observations lead us to the conclusion that this is mainly due to the smoothing effect of CuReD described in Section 2.2.1.

First, the SR of CuReD with the full mapping is lower than the Strehl with interpolation mapping (Section 4.2 and the right plot of Fig. 5). We think the reason is that the full mapping 'un-does' the smoothing introduced by the CuReD algorithm.

Secondly, in simulation we measured the SR obtained with a modified LSE reconstructor: before sending the commands to the simulated DM, we applied the same smoothing as observed for CuReD. As shown in the right plot of Fig. 5 this smoothing improves the SR; the curves are obtained with the bicubic DM interpolation but the behaviour with the bilinear or Gaussian DM is similar.

It is known that LSE is not the optimal control algorithm and that performance can be improved by using regularization, for example with the minimum mean square error or with the maximum a-posteriori approach, see for example (Flicker, Rigaut & Ellerbroek 2000; Le Louarn 2002; van Dam, Le Mignant & Macintosh 2004; Petit et al. 2005; Neichel et al. 2010). With such a procedure, additional knowledge is built into the control matrix about the expected shape that the DM needs to correct. For example, in open loop the DM commands are expected to match a wavefront distortion caused by a Kolmogorov turbulence, which improves the result. Seemingly, the smoothing property of CuReD has a similar effect.

6 CONCLUSIONS

Using the CANARY instrument we have tested two novel wavefront reconstructors, CuReD and HWR.

We have developed three methods for mapping the CuReD or HWR output into the DM actuator commands: *full mapping*, *identity mapping* and *interpolation mapping*. The first one is an MVM-like

algorithm and is too slow for large AO systems, whereas the latter two are much faster and are suited for the ELTs.

We found out that with the identity or interpolation mapping, CuReD runs stably only if the feedback loop is operated as a leaky integrator, whereas HWR is stable with the conventional integrator control loop. We also found out that CuReD has a smoothing effect on the output wavefront, whereas HWR can reconstruct the wavefront accurately, preserving all spatial frequencies.

We used the CANARY TelSim to study the performance of both algorithms. The SR obtained with HWR is slightly lower than that of LSE. The SR of CuReD is slightly higher than that of LSE if using the interpolation mapping, whereas with the full mapping it is slightly lower. Our investigation and additional tests with a computer simulation suggest that the higher Strehl is due to the smoothing effect of CuReD.

We have tested both reconstructors extensively on-sky. They performed well with both full and interpolation mapping. CuReD achieved a similar SR as LSE, whereas HWR was slightly lower.

We compare the findings with the results from a computer simulation and they are in good agreement.

The CANARY TelSim was crucial for these studies: without it the investigation of algorithms' performance would not have been possible. It was also very helpful to use the concept of real-time simulation and to connect the simulation software to the same RTC as was used with CANARY.

With these results CuReD and HWR have passed the first real-life test, including an on-sky validation. However, in order to gain confidence in their suitability for ELTs it is now crucial to test them on systems with more subapertures. In particular one needs to study their sensitivity to noise and confirm the speed-up compared to the MVM method.

ACKNOWLEDGEMENTS

This research has made use of the SIMBAD database, operated at CDS, Strasbourg, France, and of the Tycho-2 catalogue by E. Høg et al. The C code for the CuReD algorithm that we used was developed and provided by Matthias Rosensteiner and Andreas Obereder (MathConsult GmbH, Linz, Austria). We also thank Matthias and Andreas for many useful discussions! We appreciate the comments on the paper draft by Aglaé Kellerer. In UK this research project is supported by the Science and Technology Facilities Council (grant no. ST/I002871/1). The French authors acknowledge the support from CNRS/INSU, Observatoire de Paris and EU OPTICON program WP1, grant agreement no. 312430.

REFERENCES

Babcock H. W., 1953, PASP, 65, 229
Basden A. G., 2014, MNRAS, 439, 2854
Basden A. G., Myers R., 2012, MNRAS, 424, 1483
Basden A. G., Butterley T., Myers R. M., Wilson R. W., 2007, Appl. Opt., 46, 1089
Bharmal N. A., Bitenc U., Basden A., Myers R., 2013, in Esposito S., Fini L., eds, Proc. Third AO4ELT Conf., A Hierarchical Wavefront Reconstruction Algorithm for Gradient Sensors. INAF – Osservatorio Astrofisico di Arcetri, Firenze, id. 48
Bitenc U. et al., 2013, in Esposito S., Fini L., eds, Proc. Third AO4ELT Conf., Tests of Novel Wavefront Reconstructors on Sky with CANARY. INAF – Osservatorio Astrofisico di Arcetri, Firenze, id. 42
Boyer C., Michau V., Rousset G., 1990, Proc. SPIE, 1271, 63
Davies R., Kasper M., 2012, ARA&A, 50, 305
de Zeeuw T., Tamai R., Liske J., 2014, The Messenger, 158, 3
Flicker R., Rigaut F., Ellerbroek B., 2000, Proc. SPIE, 4007, 4007
Gendron E. et al., 2011A&A, 529, L2
Kasper M. et al., 2010, Proc. SPIE, 7735, 77352E
Le Louarn M., 2002, MNRAS, 334, 865
Macintosh B. A. et al., 2014, Proc. SPIE, 9148, 91480J-1
Myers R. M. et al., 2008, Proc. SPIE, 7015, 70150E
Neichel B., Rigaut F., Bec M., Garcia-Rissmann A., 2010, in Clénet Y., Conan J.-M., Fusco T., Rousset G., eds, Proc. 1st AO4ELT Conf., Adaptive Optics for Extremely Large Telescopes. EDP Sciences, Les Ulis, id. 02010
Osborn J. et al., 2014, MNRAS, 441, 2508
Petit C., Conan J.-M., Kulcsár C., Raynaud H.-F., Fusco T., Montri J., Chemla F., Rabaud D., 2005, Proc. SPIE, 5903, 59030P
Pham L., 2013, Masters thesis, Univ. Victoria
Poyneer L. A., Gavel D. T., Brase J. M., 2002, J. Opt. Soc. Am. A, 19, 2100
Poyneer L. A. et al., 2014, Proc. SPIE, 9148, 91480K
Rosensteiner M., 2011, J. Opt. Soc. Am. A, 28, 2132
Rosensteiner M., 2012, J. Opt. Soc. Am. A, 29, 2328
Shatokhina I., Obereder A., Rosensteiner M., Ramlau R., 2013, Appl. Opt., 52, 2640
Sivo G. et al., 2014, Opt. Expr., 22, 23565
Spyromilio J., Comerón F., D'Odorico S., Kissler-Patig M., Gilmozzi R., The Messenger, 133, 2
van Dam M. A., Le Mignant D., Macintosh B. A., 2004, Appl. Opt., 43, 5458
Zhariy M., Neubauer A., Rosensteiner M., Ramlau R., 2011, Inverse Probl. Imaging, 5, 893

APPENDIX A

Here, we explain how we use the interaction matrix to estimate the actuator positions with respect to the subaperture grid.

With a perfect alignment the DM actuators are positioned at subaperture corners (Fried geometry). Our simulation shows that the gradient obtained by poking an actuator points in the direction of that actuator within a few degrees even if the actuator is significantly (by up to 25 per cent of the subaperture size) displaced from the subaperture corner. This holds as long as at least 3/4 of subaperture's surface is illuminated and the non-illuminated area is symmetrical with respect to the subaperture's diagonal that is closest to the poked actuator.

Thus we obtain an actuator position by poking the actuator and intersecting the gradient lines from the subapertures around it, as demonstrated in the left plot of Fig. A1. A similar method has been used for calibration of the Raven instrument as described by Pham (2013). After rejecting the non-symmetrically illuminated subapertures, there are 20 actuators for which the position can be determined, as shown in the right plot of Fig. A1. For four of

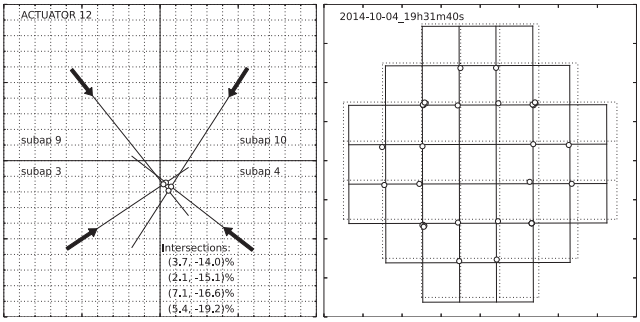

Figure A1. Left: retrieving the actuator position (circles) from the slopes in the interaction matrix (arrows). Right: the measured actuator positions (circles) and the grid fitted to them (full lines); the dotted lines represent the subaperture grid.

them the position can be determined from four different pairs of subapertures; by comparing the four results we estimate that the resolution of an actuator position measurement is about 3 per cent of the subaperture size.

We fit an actuator grid to the measured actuator positions with five free parameters that describe its relation to the subaperture grid: displacement (x and y), magnification (x and y) and rotation around the centre. Separate x and y magnification factors account for different incidence angles of the light beam which is about 75° to the x-axis and 90° to the y-axis. The quality of the fit using a common magnification factor was significantly worse.

From the fit result we obtain the positions of all actuators with respect to the subaperture grid, which are used for the interpolation mapping as explained in Section 2.2.2.

This paper has been typeset from a TEX/LATEX file prepared by the author.